

GRAPPA-accelerated Readout-Segmented EPI for High Resolution Diffusion Imaging

S. J. Holdsworth¹, S. Skare¹, R. D. Newbould¹, A. Nordell², and R. Bammer¹

¹Department of Radiology, Stanford University, Palo Alto, CA, United States, ²Hospital Physics, Karolinska University Hospital, Stockholm, Sweden

Introduction: Readout-segmented (RS)-EPI (1) has been suggested as an alternative approach to EPI for high resolution diffusion-weighted imaging (DWI). In RS-EPI scheme, segments of k -space are acquired along the readout direction. This reduces geometric distortions due to the decrease in echo spacing. Here we demonstrate that a combination of the RS-EPI k -space trajectory and parallel imaging results in high resolution T2-weighted and diffusion-weighted images with minimal geometric distortions. Clinical RS-EPI DWI images delineate tumors near the auditory canals, nasal cavity, and the brain stem - areas traditionally difficult for EPI-based trajectories to image with high quality. DTI images are also acquired and compared with GRAPPA-accelerated EPI. The short scan times made possible through the use RS-EPI may make it a useful alternative sampling strategy for high resolution diffusion imaging.

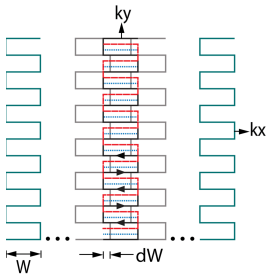


Fig. 1: k -space trajectories for the RS-EPI sequence. K -space is filled with an odd number of separate blinds, B , (indicated by green, grey, and black) of a given blind width, W , and overlapping factor, $OF = dW/W$.

Materials & Methods: Fig. 1 shows the k -space trajectory for RS-EPI. For each repetition, each (partial-Fourier encoded) segment or 'blind' may be acquired with several interleaves, each accompanied by an extra navigator for phase correction. Depending upon the number of blinds chosen, the blind width, W ; and the target resolution in the readout-direction - the amount the blinds may overlap, dW , is described by the *overlapping factor*, OF . In the case of parallel imaging, only the central blind is acquired with GRAPPA-acceleration factor $R = NEX$. This blind can be used for referenceless ghost parameter estimation (2) and GRAPPA (3-4) calibration, values which are applied to all other ($b = 0$ and DW blinds). The RS-EPI sequence was developed for a 3T whole-body GE EXCITE system (Milwaukee, WI, USA).

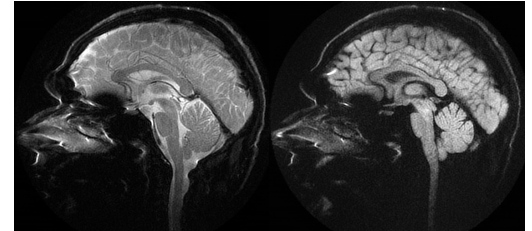


Fig. 2: RS-EPI (left) $b = 0$ and (right) $b = 1000 \text{ s/mm}^2$ (isotropic tetrahedral encoding) coronal images. Imaging parameters were: FOV=26 cm, slice thickness = 5 mm, $N = 288$, $R = NEX = 3$, 9 blinds, $W = 64$, $OF = 50\%$, TR/TE = 3s/62ms, scan time = 6:48 min.

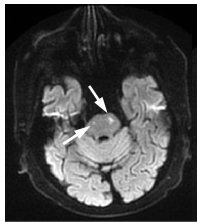


Fig. 4: RS-EPI isotropic DWI dataset (x, y, z direction, $b = 1000 \text{ s/mm}^2$) acquired with 5 blinds, an in-plane target resolution = 192×192 , $W = 64$, slthck = 5mm, $R (= NEX) = 2$, 18 overscans, TR = 3s, and a total scan time = 2 min.

An 8-channel head coil and a high-performance gradient system (40 mT/m, SLR = 150 mT/m/s) was used. Patient studies were IRB approved and volunteers signed consent forms. For volunteer studies, axial, sagittal, and coronal RS-EPI $b = 0$ and $b = 1000 \text{ s/mm}^2$ images were acquired at a target resolution of 288×288 . Imaging parameters were: FOV = 24 cm; a slice thickness = 5 mm; TR/TE = 3 s/68 ms; $R = 3$; $NEX = R$; 9 blinds of width 64 ($OF = 50\%$); isotropic tetrahedral encoding with $b = 1000 \text{ s/mm}^2$, resulting in a scan time of 6:48 min for each of the three scan planes. For patient studies, a RS-EPI-DW acquisition was performed in a patient with a brain stem cavernoma and with a stroke in the brain stem. The dataset used a 192×192 in-plane target resolution; a GRAPPA-acceleration factor $R = NEX = 2$; five blinds of width 64 ($OF = 40\%$); a FOV = 24cm; slice thickness = 4 mm; partial-Fourier encoding with $N_o = 18$; TR/TE_{min} = 3s/67ms; and a total scan time of 2 mins. The DWI images were acquired using a $b = 0 \text{ s/mm}^2$ complemented by three $b = 1000 \text{ s/mm}^2$ images (x, y , and z direction), resulting in a scan time of 2 min. For comparison, a standard single-shot (ss)EPI DW image was acquired with an in-plane target resolution of 128×128 . To compare the performance of GRAPPA-accelerated EPI with RS-EPI, diffusion-tensor images (DTI) were acquired on a volunteer with an equivalent scan time. Both datasets used an in-plane target resolution of 288×288 , a FOV = 24 cm, slice thickness of 5 mm, and $R = NEX = 3$. For the RS-EPI dataset, 7 blinds were acquired with a blind width of 64 ($OF = 35\%$). For the EPI dataset, 7 repetitions of the diffusion scheme were implemented. Diffusion weighting with a $b = 1000 \text{ s/mm}^2$ was carried out along 15 isotropically distributed directions, complemented by three $b = 0 \text{ s/mm}^2$ images. With a TR of 3 s for both datasets, the total scan time was 19 minutes. Isotropic DWI, fractional anisotropy maps; and directionally encoded color maps are presented. An FSE sequence acquired at the same target resolution was also acquired for geometric reference.

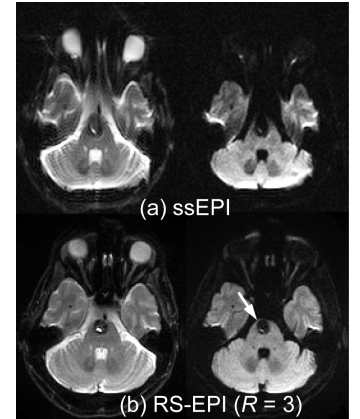
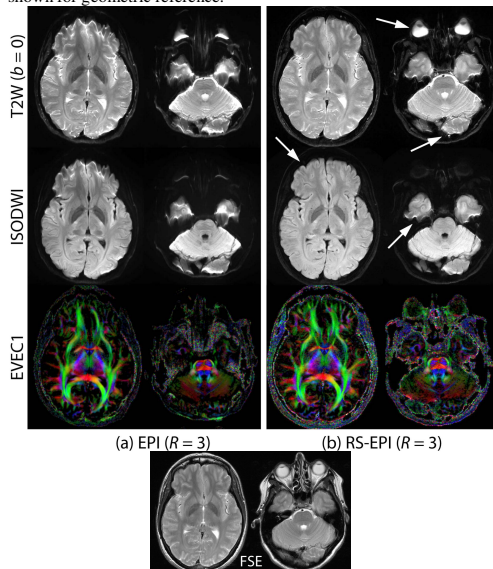


Fig. 3: T2w ($b=0$) and isotropic DW datasets (x, y, z direction, $b=1000 \text{ s/mm}^2$) from a brain stem cavernoma patient. (a) ssEPI acquired at a target resolution of 128×128 . (b) RS-EPI image acquired with a target resolution of 192×192 , $R = NEX = 3$, and 5 blinds ($W = 64$, $OF = 40\%$). A FOV = 24 cm, slthck = 4 mm, partial-Fourier encoding with 18 overscans, and a TR = 3 s were used, resulting in a scan time of 2 min (RS-EPI) and 0:15 s (ssEPI).

Fig. 5: GRAPPA-accelerated (a) EPI and (b) RS-EPI DTI datasets acquired on a healthy volunteer (three $b = 0 \text{ s/mm}^2$ and 15 directions with $b = 1000 \text{ s/mm}^2$). Imaging parameters were: $R = NEX = 3$, a target resolution of 288×288 , partial Fourier encoding with $N_o = 18$, FOV = 24 cm, slice thickness = 5mm, and a TR = 3s. b) used 7 blinds ($W = 64, OF = 36\%$) and a) 7 repetitions of the DTI sequence to achieve an equivalent scan time (19 min). A 288×288 FSE image is shown for geometric reference.



For the RS-EPI dataset, 7 blinds were acquired with a blind width of 64 ($OF = 35\%$). For the EPI dataset, 7 repetitions of the diffusion scheme were implemented. Diffusion weighting with a $b = 1000 \text{ s/mm}^2$ was carried out along 15 isotropically distributed directions, complemented by three $b = 0 \text{ s/mm}^2$ images. With a TR of 3 s for both datasets, the total scan time was 19 minutes. Isotropic DWI, fractional anisotropy maps; and directionally encoded color maps are presented. An FSE sequence acquired at the same target resolution was also acquired for geometric reference.

Results: In Fig. 2, RS-EPI $b = 0 \text{ s/mm}^2$ and isotropically weighted $b = 1000 \text{ s/mm}^2$ images acquired at an in-plane target resolution of 0.8 mm^2 (matrix size 288×288) present with little blurring and distortion. DW images of the cavernoma patient in Fig. 3 show that while the standard 128×128 ssEPI $b = 0 \text{ s/mm}^2$ and isotropically weighted $b = 1000 \text{ s/mm}^2$ images (Fig. 3a) suffer from substantial distortion and blurring, the RS-EPI images (Fig. 3b) clearly delineate the brain stem cavernoma. The improvement in geometric distortion properties is particularly noticeable regions around the nasal cavity, and areas adjacent to the hemorrhagic lesions. Fig. 4 shows an isotropic RS-EPI-DW dataset depicting a dataset of a patient suffering from a stroke in the brain stem. Fig. 5 shows two slices from each of the GRAPPA-accelerated EPI and RS-EPI DTI datasets acquired with an in-plane target resolution of 288×288 with the same scan time (19 min). While the additional repetitions of the EPI dataset yield images with high SNR, considerable geometric distortion remain at the level of the eyes, nasal cavities, auditory canals, and the occipital and frontal lobe.

Summary: It is demonstrated that the combination of parallel imaging and the RS-EPI k -space trajectory gives resulting in images with reduced geometric distortions and exquisite spatial resolution at 3T. This method allows the clear delineation of structures and pathology in the lower parts of the brain, areas traditionally difficult for EPI to acquire with reliable image quality.

References: 1) Porter D et al. ISMRM 2004;442. 2) Nordell A et al. ISMRM 2007;1833. 3) Griswold MA, et al. MRM 2002;47:1202-1210. 4) Qu P, et al. JMR 2005;174(1):60-67. **Acknowledgements:** This work was supported in part by the NIH (2R01EB002711, 1R21EB006860), the Center of Advanced MR Technology at Stanford (P41RR09784), the Lucas Foundation, the Oak Foundation, and the Swedish Research Council (K2007-53P-20322-01-4). The authors are grateful to Anne Sawyer and Sandra Rodriguez for providing assistance with the patient studies. I would like to thank Bronwen Holdsworth for her inexhaustible help with proofreading.